N-H group of an ethylenediamine chelate ring. Such an interaction is impossible in the L enantiomer.[19] X-ray crystallography of the complex (citrato)(triethylenetetramine)cobalt(III) shows a three-point attachment of the citrato ligand. It is coordinated via the hydroxyl group and one of the oxygen atoms of the central carboxyl group, and in addition, an internal hydrogen bond between one of the terminal carboxyl groups, and the tetraamine ligand is formed.[20] Hydrogen bond formation between the side chain carboxylate of aspartic acid chelated in (aspartato)bis(ethylenediamine)cobalt(III) and one of the amino ligands was invoked to explain the asymmetric deuteration of the α-carbon of the amino acid ligand.[21]

Acknowledgment. Support of this work by National Institutes of Health Grant No. GM13638-17 and also National Science Foundation Grant Nos. GP-28142 and CHE77-08810 is gratefully acknowledged.

Registry No. $[(NH_3)_5Ru^{II}NH_2CH_2CONH_2](PF_6)_2$, 86885-72-5; $[(NH_3)_5Ru^{II}NH_2CH_2CONHCH_2CH_3](PF_6)_2$, 86885-74-7; $[(NH_3)_5Ru^{II}NH_2CH_2CONHCH_2COOH](PF_6)_2$, 86885-77-0; $[(NH_3)_5Ru^{II}NH_2CH_2CONHCH_2CONH_2](PF_6)_2$, 86885-79-2; $[(NH_3)_5Ru^{II}NH_2CH_2CONHCH_2COOCH_2CH_3](PF_6)_2$, 86885-81-6; $[(NH_3)_5Ru^{III}NH_2CH_2CONH_2]^{3+}$, 86885-82-7; $[(NH_3)_5Ru^{III}NH_2CH_2CONHCH_2CH_3]^{3+}$, 86885-83-8; $[(NH_3)_5Ru^{III}NH_2CH_2CONHCH_2COO^-]^{2+}$, 86885-84-9; $[(NH_3)_5Ru^{III}NH_2CH_2CONHCH_2CONH_2]^{3+}$, 86885-85-0; $[(NH_3)_5Ru^{III}NH_2CH_2CONHCH_2COOC_2H_5]^{3+}$, 86885-86-1; (glycinamide-*N*,*O*)tetraammineruthenium(III), 85320-45-2; (*N'*-ethylglycinamide-*N*,*O*)tetraammineruthenium(III), 85320-46-3; (glycylglycinato-*N*,*O*)tetraammineruthenium(III), 85320-47-4; (glycylglycinamide-*N*,*O*)tetraammineruthenium(III), 86885-87-2; (ethyl glycylglycinate-*N*,*O*)-tetraammineruthenium(III), 86885-88-3; (glycinamide-*N*,*N'*)tetraammineruthenium(III), 86885-89-4; (glycylglycinato-*N*,*N'*)tetraammineruthenium(III), 86885-90-7; (glycylglycinamide-*N*,*N'*)-tetraammineruthenium(III), 86885-91-8; (ethyl glycylglycinate-*N*,*N'*)tetraammineruthenium(III), 86885-92-9.

Contribution from the Central Research Institute for Chemistry, Hungarian Academy of Sciences, H-1525 Budapest, Hungary, and Department of Chemistry, The University of Texas at Arlington, Arlington, Texas 76019

A New μ-Peroxo Cobalt(III) Complex: Kinetics and Mechanism of the Oxygenation of the Bis(*o*-phenylenediamine)cobalt(II) Ion

SÁNDOR NÉMETH[1a,b] and LÁSZLÓ I. SIMÁNDI*[1a,c]

Received February 10, 1983

Methanol solutions of cobalt(II) salts containing a large excess of *o*-phenylenediamine (OPD) absorb 0.5 mol of dioxygen/mol of cobalt, leading to the formation of the purple (μ-peroxo)bis[bis(*o*-phenylenediamine)cobalt(III)] ion. Subsequent slower O_2 uptake is accompanied by ligand oxidation. Stopped-flow kinetic results are consistent with a two-step oxygenation mechanism of the bis(*o*-phenylenediamine)cobalt(II) ion, the only reactive species in the $Co(OPD)_n^{2+}$ system (n = 1-6). The rate constant for the reversible first step, k_1, is 47.0 ± 7.0 mol^{-1} dm^3 s^{-1}, and k_{-1}/k_2 = (8.0 ± 2.0) × 10^{-6} mol dm^{-3}. Kinetic analysis also provides the first two stability constants K_1 = 14.0 ± 3.0 and K_2 = 4.5 ± 1.3 mol^{-1} dm^3, not available from other sources.

Introduction

We have recently reported that *o*-phenylenediamine (OPD) can be catalytically oxidized by molecular O_2 in the presence of Co^{2+} salts. The product of oxidation depends on the type of solvent used.[2] In acetone, 2,2-dimethyl-2*H*-benzimidazole is formed via 2,2-dimethyl-2,3-dihydrobenzimidazole with good selectivity.

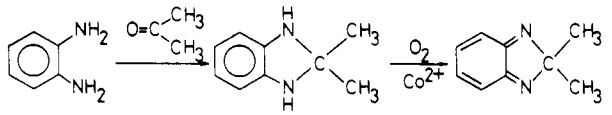

In nonreactive solvents, 2,3-diaminophenazine (DAP) is the only product.

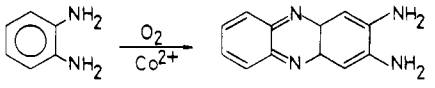

We have found that the initial stages of these catalytic reactions consist of the oxygenation of the OPD/cobalt(II) system. In this paper, we report on the nature of oxygen complexes formed and describe the kinetics and mechanism of the dioxygen absorption process.

Results and Discussion

Stoichiometry of Oxygenation. Under anaerobic conditions, various cobalt(II) salts have been reported to form a series of OPD complexes of the formula $Co(ODP)_nX_2$, where n = 1, 2, ..., 6 and X is a univalent anion.[3-6] No data are available for the stabilities of these complexes. Their sensitivity to dioxygen has been noted, but there is no information concerning their reactions with O_2.

Addition of cobalt(II) perchlorate to a solution of OPD in MeOH saturated with dioxygen leads to immediate appearance of an intense purple color. Successive UV-vis spectra of the system are shown in Figure 1. Initially, up to spectrum 4, the absorbance increases monotonically, reflecting the progress of a single reaction. The color is due either to a single species or to a set of products in a constant ratio, which follows from the constant ratio of absorbances at any selected wavelength. After the solution is allowed to stand, a new band appears at 440 nm, indicating the formation of DAP, the product of catalytic OPD oxidation. The spectra exhibiting the 440-nm band (e.g., spectrum 5 in Figure 1) are superpositions of spectrum 4 and of the spectrum of DAP, up to at least 50% conversion of OPD to DAP.

The final spectrum 4, preceding the noticeable start of OPD oxidation, is independent of the cobalt(II) salt used (X may be NO_3^- or Cl^-, too) and of the type of solvent employed (MeOH, THF, acetone). Beer's law was found to be valid in the 400-800-nm range at various initial CoX_2 concentrations.

The absorbance of the OPD/Co^{2+} system under O_2-free N_2 was found to be negligible compared with the spectra shown in Figure 1.

(1) (a) The University of Texas at Arlington. On leave of absence from Central Research Institute for Chemistry, Hungarian Academy of Sciences. (b) R. A. Welch postdoctoral fellow. (c) Visiting professor.
(2) Németh, S.; Simándi, L. I. *J. Mol. Catal.* **1982**, *14*, 241-246.
(3) Duff, E. J. *J. Chem. Soc. A* **1968**, 434-437, 836-837.
(4) Marks, D. R.; Philips, D. J.; Redfern, J. P. *J. Chem. Soc. A*, **1967**, 1464-1469; *Ibid.* **1968**, 2013-2017.
(5) Duff, E. J. *J. Inorg. Nucl. Chem.* **1970**, *32*, 2106-2107.
(6) Kakazai, B. J. A.; Melson, G. A. *Inorg. Chim. Acta* **1970**, *4*, 360-364.

0020-1669/83/1322-3151$01.50/0

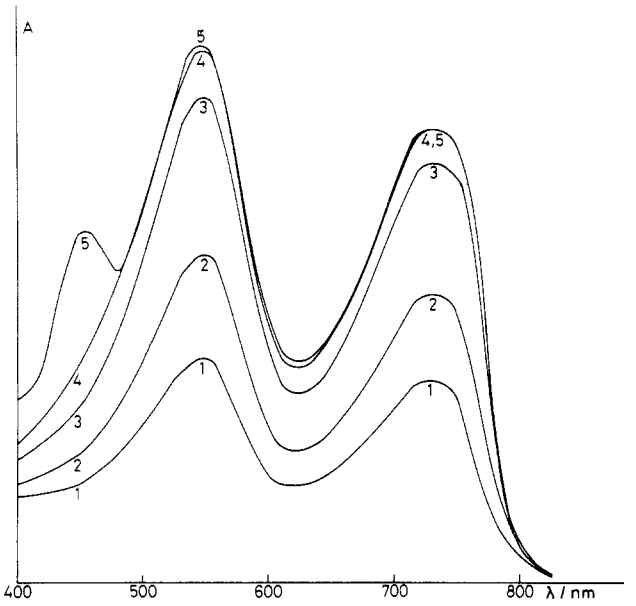

Figure 1. Spectral change in the $Co^{2+}/OPD/O_2$ system with time (solvent MeOH, T = 25 °C, $[Co]_0 = 5 \times 10^{-5}$ mol dm^{-3}, $[OPD]_0 = 4 \times 10^{-2}$ mol dm^{-3}, $[O_2]_0 = 2 \times 10^{-3}$ mol dm^{-3}). Times after mixing: curve 1, 3 min; curve 2, 6 min; curve 3, 10 min; curve 4, 12 min; curve 5, 30 min.

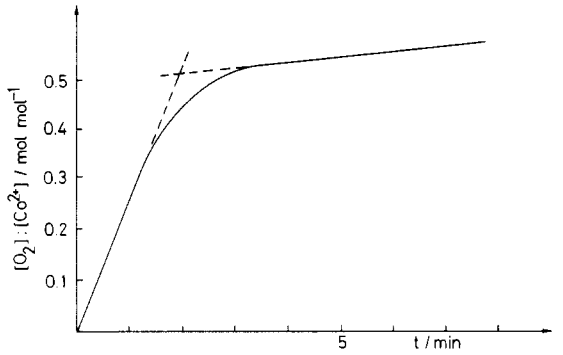

Figure 2. Oxygen uptake by the Co^{2+}/OPD system (solvent MeOH, T = 25 °C, $[Co]_0 = 5 \times 10^{-2}$ mol dm^{-3}, $[OPD]_0$ = 0.1 mol dm^{-3}, $P_{O_2} \approx 1$ atm).

The volumetric O_2-absorption curves of solutions containing cobalt(II) perchlorate and OPD in ratios of 1:2–1:10 show two distinct sections (Figure 2). Extrapolation of the nearly linear sections reveals that the initial, faster reaction corresponds to a dioxygen uptake of 0.5 mol of O_2/mol of Co^{2+}. The same molar ratio is observed if independently prepared[4,5] solid $Co(OPD)_2X_2$ or $Co(OPD)_3X_2$ complexes are suspended in benzene or toluene and exposed to dioxygen. Under such conditions, the original pink compounds are converted to the same purple complex described above. Solutions of the purple complex react with sulfite and thiosulfate ions. Titration with these reductants has shown the presence of 0.5 mol of O_2/mol of cobalt(II), supporting the results of volumetric experiments. (O_2 was assumed to be reduced to H_2O.) The UV–vis spectra recorded after dissolution of the solid complexes in MeOH under O_2 are quantitatively identical with spectrum 4 of Figure 1. These facts strongly indicate that the purple complex contains all the cobalt present in the reacting systems.

Nature of the Purple Complex. A question of importance is the number of OPD ligands in the purple complex. Identical molar amounts of $Co(OPD)_nX_2$, with n = 2 or 3, were oxygenated in benzene/THF suspension, and the purple product was filtered off and dissolved in MeOH. Spectrophotometric analysis revealed that identical amounts of the purple complex formed in both cases. When $Co(OPD)X_2$ was subjected to the same treatment, less than half of the purple complex was formed. Rapid addition of excess OPD to the MeOH solutions brought about no change in the absorbance when n = 2 or 3. However, for n = 1, this operation produced doubling of the intensity, the spectrum becoming identical with those found for n = 2 and 3. These facts indicate that the purple complex is formed from the $Co(OPD)_2^{2+}$ ion, which is the only complex in the system reactive toward dioxygen.

Gas chromatographic determination of OPD in the purple complex is possible by utilizing the conversion of coordinated OPD to 2,2-dimethyl-2*H*-benzimidazole with acetone.[2,7] The solid purple complex, prepared freshly by precipitation from MeOH solution, was dissolved in acetone, and the product was analyzed by GLC. The amount of OPD recovered in the form of 2,2-dimethyl-2*H*-benzimidazole was 1.8–1.9 mol/mol of cobalt.

It is conceivable that the purple complex contains some oxidized derivative of OPD rather than OPD itself. The known oxidation product DAP does form complexes with cobalt(II) ions; however, their UV–vis spectra are quite different from that of the purple complex, which eliminates DAP as a ligand. *o*-Benzoquinone diimine, which is known to be an intermediate in some stoichiometric oxidations of OPD (e.g., by iron(III) complexes), is another possible ligand, owing to its known ability to bond to transition-metal ions. Upon addition of cobalt(II) salts to a freshly prepared dilute solution[8-11] of *o*-benzoquinone diimine under N_2, deep red complexes are formed in both the absence and presence of OPD, which turn brownish in air. The spectra of these solutions do not resemble that of the purple compound; consequently, *o*-benzoquinone diimine is not a ligand in that complex.

The infrared spectrum of the purple compound, precipitated with CCl_4 from an O_2-saturated MeOH solution of $Co(OPD)_2(ClO_4)_2$, shows that the bands characteristic of coordinated OPD are unchanged in the purple complex, indicating no chemical transformation of this ligand. The same is true for $Co(OPD)_2Cl_2$ and $Co(OPD)_2(NO_3)_2$. It was not possible to record the resonance Raman spectrum of the purple compound as it exploded upon laser illumination. When the purple complex is formed in solution, no ESR-active species can be detected; consequently, no superoxo complexes, either mono- or binuclear, are formed in detectable amounts in contrast to the behavior of bis(aliphatic diamine)cobalt(II) complexes.[12] The $Co(OPD)_n^{2+}$ ions are also ESR inactive, owing to rapid relaxation.

The polarogram of the purple complex in 50% MeOH–water consists of a single wave with $E_{1/2}$ = 1.080 V vs. SCE, which is higher than would be expected if the central ion were cobalt(III).

The purple complex is substitutionally very labile: it is instantaneously converted to other colored species upon the addition of ligands such as Ph_3P, RNC, or R_3N. It is also rapidly decomposed by strong acids, yielding DAP and OPD in a molar ratio of ca. 2:1, even under N_2. Reducing agents such as $S_2O_3^{2-}$, SO_3^{2-}, or hydrazine make the purple color disappear. GLC of the reduced solutions reveals the presence of 2 mol OPD/mol of cobalt.

The observations relating to the nature of the purple complex permit its formulation as a binuclear μ-peroxo compoud $[L(OPD)_2Co{-}O_2{-}Co(OPD)_2L](ClO_4)_4$. In coordinating solvents,

(7) Németh, S.; Simándi, L. I. *J. Mol. Catal.* **1982**, *14*, 87–93.
(8) Lee, H. Y.; Adams, R. N. *Anal. Chem.* **1962**, *34*, 1587–1590.
(9) Nogami, T.; Hishida, T.; Shirota, Y.; Mikawa, H. *Chem. Lett.* **1974**, 293–296.
(10) Nogami, T.; Hishida, T.; Shirota, Y.; Mikawa, H.; Nagakura, S. *Bull. Chem. Soc. Jpn.* **1974**, *47*, 2103–2106.
(11) Nogami, T.; Hishida, T.; Yamada, M.; Mikawa, H.; Shirota, Y. *Bull. Chem. Soc. Jpn.* **1975**, *48*, 3709–3714.
(12) Khare, G. P.; Lee-Ruff, E.; Lever, B. P. *Can. J. Chem.* **1976**, *54*, 3424–3429.

the corresponding tetrapositive (μ-peroxo)bis[bis(*o*-phenylenediamine)cobalt(III)] ion is the predominant species with L = solvent. Ion-pair formation with perchlorate ions is expected owing to its high positive charge. The nature of the sixth ligand around cobalt seems to depend on the anion of the cobalt(II) salt used. In the case of $Co(SCN)_2 \cdot 3H_2O$ as starting material, the IR spectrum of the solid μ-peroxo complex provides direct evidence for coordination of the SCN^- ligand. With ClO_4^- as the anion, no such evidence is available and the sixth coordination sites are probably occupied by water molecules. Preliminary results of μ-peroxo cobalt complex formation in the presence of Ph_3P clearly demonstrate the presence of this ligand in the coordination sphere. The inherent instability of the μ-peroxo complex with respect to OPD oxidation has prevented us from obtaining reliable elemental analyses.

Oxygenation of the purple complex is irreversible at room temperature; no deoxygenation is possible by flushing with an inert gas or by evacuation. However, heating at 120–140 °C under N_2 produces ca. 50% water and ca. 25% O_2 (on the basis of the μ-peroxo structure), as measured by mass spectrometry.

Kinetics and Mechanism of Oxygenation. The formation of the μ-peroxo complex should apparently consist of two consecutive steps, which is the usual assumption for similar systems.[13-17] In view of the overall irreversibility, we proposed the following scheme of oxygenation:

$$Co(OPD)_2^{2+} + O_2 \underset{k_{-1}}{\overset{k_1}{\rightleftharpoons}} [Co(OPD)_2O_2]^{2+} \quad (1)$$

$$[Co(OPD)_2O_2]^{2+} + Co(OPD)_2^{2+} \xrightarrow{k_2} [(OPD)_2Co{-}O_2{-}Co(OPD)_2]^{4+} \quad (2)$$

As the μ-peroxo complex contains 2 molecules of OPD/atom of cobalt, we assume that only $Co(OPD)_2^{2+}$ is reactive toward dioxygen. The Co^{2+}/OPD system involves the successive equilibria

$$Co(OPD)_{n-1}^{2+} + OPD \underset{}{\overset{K_n}{\rightleftharpoons}} Co(OPD)_n^{2+} \quad (3)$$

with $n = 1, 2, ..., 6$. The known lability of cobalt(II) implies that the equilibria in (3) are very rapid; thus, the formation of $Co(OPD)_2^{2+}$ can be regarded as a preequilibrium.

The validity of the scheme (1)–(3) has been confirmed by kinetic experiments that will be outlined in some detail.

As the absorbance of the Co^{2+}/OPD system in the absence of O_2 is negligible compared with that under dioxygen, the oxygenation reaction can be readily followed anywhere in the 450–750-nm range by using conventional or stopped-flow spectrophotometry. The procedure employed was to mix O_2-saturated solutions of cobalt(II) perchlorate and OPD, generally at a mole ratio of 1 to 10^2–10^3, in a stopped-flow device and to monitor the buildup of the μ-peroxo complex at a selected wavelength. If the formation of $Co(OPD)_2^{2+}$ is much faster than its subsequent oxygenation, kinetic data for the latter reaction can be obtained without tedious anaerobic operations, which are the source of various errors. This technique has been previously used for studying the oxygenation of cobaloxime(II).[18]

The rapid establishment of preequilibria 3 was confirmed by concentration-jump experiments with two-stage mixing,

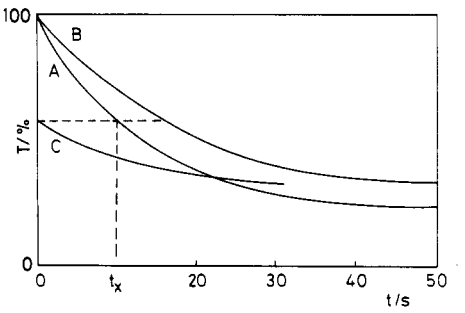

Figure 3. Stopped-flow traces for the oxygenation of the Co^{2+}/OPD system: A, undiluted trace; B, diluted trace; C, prereacted trace (see text).

illustrated in Figure 3. Stopped-flow traces A and B refer to oxygenation after one-stage mixing of solutions, with concentrations $[Co^{2+}]_1$ and $[OPD]_1$ for trace A and $^1/_2[Co^{2+}]_1$ and $^1/_2([OPD]_1 + [OPD]_2)$ for trace B. Apparently, trace B is also that of solution A mixed in a second stage with an OPD solution of $[OPD]_2$. Trace C was recorded after just that operation: solution A was prereacted with O_2 for ca. 10 s (t_x in Figure 3) and then mixed in the second stage with a solution of $[OPD]_2$. Had there been any time lag in the readjustment of equilibria 3 after the second mixing stage, one would have expected trace C to coincide with, and slowly deviate from, trace A. What is actually observed is that trace C starts at the transmission value expected for solution A after a reaction time of t_x and perfectly coincides with the section of trace B lying to the right of that % T value. This implies that dilution of reacting solution A merely halves the concentration of the μ-peroxo complex and its further accumulation rate occurs exactly as required by the new OPD concentration. In other words, equilibria 3 are established very rapidly relative to the oxygenation of $Co(OPD)_2^{2+}$, whose concentration is at all times determined by the set of K_n defined by eq 4. This behavior has been confirmed for a variety of compositions with different OPD and cobalt(II) concentrations.

$$K_n = \frac{[Co(OPD)_n^{2+}]}{[Co(OPD)_{n-1}^{2+}][OPD]} \quad (4)$$

According to ESR and UV–vis spectroscopic tests, no intermediate is detectable during oxygenation; consequently, the concentration of $[Co(OPD)_2O_2]^{2+}$ is negligible. Application of the steady-state approach to eq 1 and 2 yields the rate expression (5), where c is the concentration of the μ-peroxo

$$\frac{dc}{dt} = k_1k_2\frac{[Co(OPD)_2^{2+}]^2[O_2]}{k_{-1} + k_2[Co(OPD)_2^{2+}]} \quad (5)$$

complex. The appropriate mass equations in combination with eq 4 convert eq 5 to rate law 6, where the subscript 0 refers

$$\frac{dc}{dt} = \frac{([Co]_0 - 2c)^2([O_2]_0 - c)}{A + B([Co]_0 - 2c)} \quad (6)$$

to initial concentrations and A and B are defined by eq 7 and 8, respectively. Here β_n are the overall stability constants. Clearly, eq 7 and 8 imply that the ratio A/B^2 should be

$$A = \frac{k_{-1}}{k_1k_2}\left(\sum_{n=0}^{6}\frac{\beta_n}{\beta_2}[OPD]^{n-2}\right)^2 \quad (7)$$

$$B = \frac{1}{k_1}\sum_{n=0}^{6}\frac{\beta_n}{\beta_2}[OPD]^{n-2} \quad (8)$$

constant regardless of the actual values of $[Co]_0$, $[O_2]_0$, and $[OPD]_T$ (cf. eq 9). As OPD was added in a 10^2–10^3-fold excess over cobalt(II) throughout the experiments, the con-

(13) Simplicio, J.; Wilkins, R. G. *J. Am. Chem. Soc.* **1967**, *89*, 6092–6095.
(14) Miller, F.; Simplicio, J.; Wilkins, R. G. *J. Am. Chem. Soc.* **1969**, *91*, 1962–1967.
(15) Wilkins, R. G. *Adv. Chem. Ser.* **1971**, *No. 100*, 111–134.
(16) McLendon, G.; MacMillan, P. T.; Havihara, M.; Martell, A. E. *Inorg. Chem.* **1975**, *14*, 1423–1425, 2322–2326.
(17) McLendon, G.; Martell, A. E. *Coord. Chem. Rev.* **1976**, *19*, 1–39.
(18) Simándi, L. I.; Savage, C. R.; Schelly, Z. A.; Németh, S. *Inorg. Chem.* **1982**, *21*, 2765–2769.

Table I. Stopped-Flow Results[a]

$[OPD]_0$, mol dm^{-3}	10^6A, mol^2 dm^{-6} s	B, mol dm^{-3} s	$10^4A/B^2$, s^{-1}	S_{av},[b]
0.10	3.5	0.10	3.5	4.4
0.15	1.7	0.07	3.5	4.7
0.20	1.0	0.05	4.0	4.2
0.25	0.77	0.045	3.8	4.3

[a] Best pairs of parameters A and B for various OPD concentrations. Each row is the average of four runs at different cobalt(II) concentrations in the range of $(3.3\text{–}10.0) \times 10^{-5}$ mol dm^{-3} ($T = 25$ °C, solvent MeOH, $[O_2] = 2 \times 10^{-3}$ mol dm^{-3}). [b] From eq 9.

Table II. Spectrophotometric Results[a]

$[OPD]_0$, mol dm^{-3}	10^6A, mol^2 dm^{-6} s	B, mol dm^{-3} s	$10^4A/B^2$, s^{-1}	S_{av},[b]
0.10	3.5	0.095	3.9	4.7
0.075	12	0.19	3.3	4.1
0.050	31	0.29	3.7	5.1
0.033	77	0.45	3.8	4.3

[a] Best pairs of parameters A and B for various OPD concentrations. Each row is the average of four runs at different cobalt(II) concentrations in the range of $(3.3\text{–}10.0) \times 10^{-5}$ mol dm^{-3} ($T = 25$ °C, solvent MeOH, $[O_2] = 2 \times 10^{-3}$ mol dm^{-3}). [b] From eq 9.

centration of free OPD was replaced by $[OPD]_T$ in all the expressions.

The validity of the rate equation (6) has been confirmed by numerical integration, using a fourth-order Runge–Kutta routine with parameters A and B selected by a simplex search procedure. The best parameters chosen were those minimizing the sum defined by eq 9. A total of 10 points were used from

$$S = \frac{1}{10}\sum_{i=1}^{10}\left|\frac{x_{i,\text{calcd}} - x_{i,\text{measd}}}{x_{i,\text{measd}}}\right| \times 100 \qquad (9)$$

each kinetic trace, and fits between calculated and experimental curves were regarded as satisfactory if the condition of $S \leq 5\%$ was fulfilled. As A and B include the OPD concentration as the only variable, the best pairs of A and B were determined from sets of four kinetic runs. In each set, four different cobalt(II) concentrations were used at a single OPD concentration. The pairs of parameters A and B obtained for different OPD concentrations are listed in Tables I and II, where each line is derived from a set of four cobalt(II) concentrations. The agreement between stopped-flow and ordinary spectrophotometric results is reasonably good. The criterion that A/B^2 should be constant at constant OPD concentration is fulfilled reasonably well, which confirms the validity of the rate equation (6). The observed kinetic behavior is consistent with the assumed reaction mechanism given by eq 1–3.

It should be emphasized that the kinetic equation (6) cannot be simplified by neglecting one of the terms in its denominator, because the resulting equations lead to strongly increased errors of curve fitting. The neglect of A implies that step 1 is irreversible, whereas $B = 0$ corresponds to a mechanism in which step 1 is a preequilibrium and step 2 is rate determining. Neither of these simplified mechanisms is consistent with the observed kinetic behavior.

Although the adequacy of the mechanism (1)–(3) has now been demonstrated, the estimation of the rate and equilibrium constants involved requires an additional procedure. The dependence of B on the OPD concentration (Figure 4) can be utilized for this objective. The decrease of B with increasing $[OPD]_0$ indicates an inverse polynomial function in the concentration range studied. The stability in solution of the

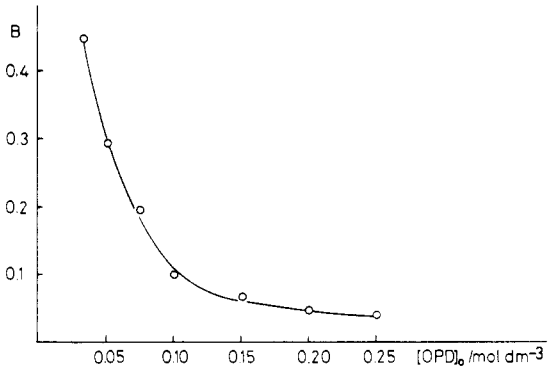

Figure 4. Dependence of B on $[OPD]_0$. The points are from Tables I and II and the curve was calculated from eq 10 with the parameters listed in Table III. Fit is within ±5%.

Table III. Rate and Equilibrium Constants[a]

k_1, mol^{-1} dm^3 s^{-1}	k_{-1}/k_2, mol dm^{-3}	K_1, mol^{-1} dm^3	K_2, mol^{-1} dm^3
47.0 ± 7.0	$(8.0 \pm 2.0) \times 10^{-6}$	14.0 ± 3.0	4.5 ± 1.3

[a] Determined from eq 10 by using the best-fit parameters $a_0 = 3.2 \times 10^{-4}$ mol^3 dm^{-9} s, $a_1 = 4.67 \times 10^{-3}$ mol^2 dm^{-6} s, and $a_2 = 2.1 \times 10^{-2}$ mol dm^{-3} s ($T = 25$ °C, solvent MeOH). For definitions of the constants, see eq 1–3.

$Co(OPD)_n^{2+}$ species is expected to decrease with increasing n. We have found that it is sufficient to consider species with $n < 3$, which implies that eq 8 can be truncated to the simpler expression (10) where $a_n = (\beta_n/\beta_2)k_1$ ($n = 0, 1, 2$). Equation

$$B = a_0[OPD]_0^{-2} + a_1[OPD]_0^{-1} + a_2 \qquad (10)$$

10 has been fitted to the B vs. $[OPD]_0$ curve of Figure 4. The best-fit values of parameters a_0, a_1, and a_2 as well as the rate and equilibrium constants derived from them are listed in Table III. The neglect of the formation of the higher complexes ($n \geq 3$) receives support from the fairly good fit between experimental points and the calculated (solid) curve in Figure 4.

No stability constants are available for cobalt(II) OPD complexes in the literature. The values of K_1 and K_2 obtained in this work point to very weak complexation. The purple μ-peroxo complex is, however, rather stable, apparently due to the stabilizing effect of the peroxo ligand. The kinetics of formation of different μ-peroxo cobalt complexes has been studied by Wilkins et al.[13–15] and by Martell et al.[16] Kinetic laws of the type in eq 6 are usually valid for these oxygenations, but sometimes they can be simplified by neglecting one of the terms in the denominator. Naturally, simplification depends on the relative values of the rate constants in steps 1 and 2. The necessity of regarding one or both steps as reversible is a complicating factor, as illustrated by our previous work on the oxygenation of cobaloxime(II).[18]

The values for k_1 are usually between 10 and 10^5 M^{-1} s^{-1}, depending on the nature of ligands coordinated to cobalt(II).[13–17] The k_1 of ca. 50 M^{-1} s^{-1} found in this work places the $Co(OPD)_2X_2$ complexes closer to the slow end of the scale. The factors governing the reactivity of cobalt(II) complexes toward dioxygen remain to be elucidated in greater detail. Work is in progress on related dioxygen-activating complexes.

Experimental Section

Reagent grade chemicals were used throughout; OPD was recrystallized twice from EtOH–H_2O.

$Co(OPD)_nX_2$ complexes were prepared under N_2, as described in the literature.[4]

Preparation of $(OPD)_2Co\text{–}O_2\text{–}Co(OPD)_2X_4$. A suspension of 2 mmol of freshly prepared $Co(OPD)_2X_2$ in 20 cm^3 of benzene–THF (10:1) was stirred under pure O_2 at atmospheric pressure in a gas

volumetric vessel. When the O_2 uptake reached 1 mmol (ca. 2 min), the dark purple powder was filtered off and dried under vacuum. IR spectra were recorded on a Hitachi Model EPI-G3 spectrometer in KBr pellets (X = ClO_4^-; bands in cm^{-1}: 3310 (s), 3260 (s), 1621 (m), 1582 (s), 1505 (vs), 1102 (vs), 780 (s), 752 (s)).

Polarograms were recorded in EtOH–H_2O (1:1). The ESR spectra were taken on a JES FE 3X instrument and the UV–vis spectra on a Beckman ACTA MIV spectrophotometer. Mass spectra of the gas phase obtained from thermal decomposition of the purple μ-peroxo complex under N_2 were recorded on an AEI MS 902 instrument.

Kinetic measurements were performed in a stopped-flow device as well as on a Beckman ACTA MIV spectrophotometer, by monitoring the buildup of the μ-peroxo complex. Data from the two sources were in good agreement in the 440–750-nm range used. The average of three to give runs was used to estimate kinetic parameters for each individual composition, the reproduciblity being ±5%. All reactions were run at 25 °C in MeOH, up to a conversion of ca. 80%. The solubility of O_2 in MeOH was taken as in ref 19.

Registry No. $[(OPD)_2Co–O_2–Co(OPD)_2](ClO_4)_4$, 87012-56-4; $Co(OPD)_2^{2+}$, 49866-76-4.

(19) Kretschmert, D. C.; Nowakowaska, J.; Weibe, R. *Ind. Eng. Chem.* **1946**, *38*, 506–609.

Contribution from the Department of Chemistry, University of Wisconsin—Madison, Madison, Wisconsin 53706

^2H NMR Spectral Studies of Intramolecular Rearrangements in Pentaborane(9)

JOSEPH A. HEPPERT and DONALD F. GAINES*

Received December 15, 1982

The rearrangement of various deuterium-labeled derivatives of pentaborane(9) in diethyl ether was studied by ^{11}B and ^2H NMR spectroscopy. Two distinct pathways for intramolecular exchange were identified at temperatures under 65 °C. One pathway allows movement from bridging positions to basal terminal positions, and a second higher energy pathway allows migration from basal terminal positions into the apex of the molecule. Exchange into and out of the apex of pentaborane appears to occur only when a substituent is one of the migrating groups. A mechanistic model for the isomerizations that conforms to the new data is suggested.

Introduction

Acid- and base-catalyzed intramolecular rearrangements are common in organic chemistry. Simple 1,2-hydride shifts and Wagner–Meerwein and Pinacole[1] rearrangements have been known for as long as 100 years. Many such acid-catalyzed rearrangements proceed via the formation of a carbonium ion and subsequent functional group migration. In cases where unfavorable orbital orientations preclude simple 1,2-shifts, intermolecular functional group transfer[2] and skeletal rearrangements[3] have been shown to operate in apparent intramolecular isomerizations. Base-catalyzed intramolecular rearrangements are historically more infrequent than acid-catalyzed reactions.[4] Consequently, the mechanisms involved in base-catalyzed rearrangements have been less exhaustively investigated.

The mechanism of isomerization of various pentaborane(9) derivatives by Lewis bases remains clouded despite the fact that the phenomenon was observed nearly 20 years ago. The first example of pentaborane rearrangement was the nearly quantitative production of 2-MeB_5H_8 from 1-MeB_5H_8 in the presence of lutidine (eq 1).[5]

$$1\text{-}MeB_5H_8 \xrightleftharpoons{2,6\text{-}Me_2(C_6H_3N)} 2\text{-}MeB_5H_8 \qquad (1)$$

Since this discovery, a wide variety of main group-substituted pentaboranes have been shown to isomerize in the presence of Lewis bases.[6] Among them are the bridge-silyl-substituted pentaboranes,[6a] which were the first compounds to demonstrate that all three positional isomers could be interconverted by Lewis base catalysts (eq 2). It was also

$$(\mu\text{-}Me_3Si)B_5H_8 \xrightarrow{Et_2O} 2\text{-}(Me_3Si)B_5H_8 \xrightleftharpoons{HMTA} 1\text{-}(Me_3Si)B_5H_8 \qquad (2)$$

determined that various derivatives could interact differently with a given Lewis base. For example, while 1-ClB_5H_8 rapidly forms 2-ClB_5H_8 in the presence of diethyl ether,[6b] only nitrogen bases (i.e., lutidine or HMTA) catalyze the conversion of 1-alkyl- to 2-alkylpentaboranes.[6c]

Early in the investigation of isomerization reactions, various mechanisms were proposed to explain the observed rearrangements. These explanations were largely derived by empirical means and attempted to deal with two major questions: What is the role of the Lewis base in isomerization, and what is the structure of the intermediate involved in the isomerization process?

Two proposals were developed for the role of the Lewis base in the isomerization of pentaborane derivatives. The first model proposed that isomerization proceeded by base deprotonation of the borane, followed by rearrangement of the borane anion, and subsequent reprotonation of the isomerized anion.[5,6d] A second proposal suggested that the base coordinated with the borane, causing sufficient distortion of the

(1) Fittig, R. *Justus Liebigs Ann. Chem.* **1860**, *114*, 54.
(2) Schleyer, P. v. R.; Lam, L. K. M.; Raber, D. J.; Fry, J. L.; McKervey, M. A.; Alford, J. R.; Cuddy, B. D.; Keizer, V. G.; Geluk, J. L.; Schlatmann, J. L. M. A. *J. Am. Chem. Soc.* **1970**, *92*, 5246–5247.
(3) Majerski, Z.; Schleyer, P. v. R.; Wolf, A. P. *J. Am. Chem. Soc.* **1970**, *92*, 5731–5733.
(4) Lowry, T. H.; Richardson, K. S. "Mechanism and Theory in Organic Chemistry"; Harper and Row: New York, 1976; pp 250–251.
(5) Onak, T. P. *J. Am. Chem. Soc.* **1961**, *83*, 2584.
(6) (a) Gaines, D. F.; Iorns, T. V. *J. Am. Chem. Soc.* **1968**, *90*, 6617–6621. (b) Gaines, D. F.; Martens, J. A. *Inorg. Chem.* **1968**, *7*, 704–706. (c) Onak, T.; Dunks, G. B.; Searcy, J. W.; Spielman, J. *Ibid.* **1967**, *6*, 1476–1471. (d) Hough, W. V.; Edwards, L. J.; Stang, A. F. *J. Am. Chem. Soc.* **1963**, *85*, 831. (e) Onak, T. P.; Gerhart, F. J.; Williams, R. E. *Ibid.* **1963**, *85*, 1754–1756. (f) Burg, A. B.; Sandhu, J. S. *Ibid.* **1965**, *87*, 3787–3788. (g) Friedman, L. B.; Lipscomb, W. N. *Inorg. Chem.* **1966**, *5*, 1952–1957. (h) Gaines, D. F.; Iorns, T. V. *J. Am. Chem. Soc.* **1967**, *89*, 3375. (i) Tucker, P. M.; Onak, T.; Leach, J. B. *Inorg. Chem.* **1970**, *9*, 1430–1441. (j) Gaines, D. F.; Iorns, T. V. *Ibid.* **1971**, *10*, 1094–1095.

0020-1669/83/1322-3155$01.50/0